Analysis of the Differential Conformational Behavior of Two Antigens of the Hepatitis A Virus through Molecular Dynamics and Physicochemical Measurements

Josep Canto,[†] Isabel Haro,[‡] Maria A. Alsina,[§] and Juan J. Perez*,[†]

Departament d'Enginyeria Quimica, ETSEIB, Technical University of Catalonia, Av. Diagonal 647, E-08028 Barcelona, Spain, Departament de Química de Pèptids i Proteïnes, IIQAB-CSIC, Jordi Girona Salgado 18-26; E-08034 Barcelona, Spain, and Departament de Fisicoquímica, Facultat de Farmacia, Universitat de Barcelona, Plaça Pius XII, s/n, E-08028 Barcelona, Spain

Received: December 9, 2002; In Final Form: April 15, 2003

The surface activity of peptides with proven antigenic activity toward the hepatitis A virus (HAV), [Glu^{114}]VP3(110−121) and [Lys^{113}]VP3(110−121), analogues of the VP3(110−121) antigen of HAV with sequence FWRGDLVFDFQV, was deduced from compression isotherm experiments. The results showed that the lysine analogue exhibits a surface area about three times smaller than that of the glutamic acid analogue. To understand whether this observed differential conformational behavior of the two peptide analogues is a characteristic feature of the peptide sequences, we carried out 10 ns molecular dynamics simulations of the two analogues in water. The results of this study confirm a differential conformational behavior of the two peptides and provide support to the hypothesis of this observed behavior as the reason for the different surface areas obtained from compression isotherm experiments.

Introduction

Synthetic peptides are appealing tools to investigate protein-related diseases without the need to use whole proteins, thus avoiding the difficulties associated with protein production. In the immune field, peptides are considered a good alternative to overcome the drawbacks that limit the use of traditional vaccines.[1,2]

Although most neutralizing and protective B cell epitopes are generally discontinuous (conformational antigenic sites) and cannot be easily mimicked by linear synthetic peptides, we previously described a continuous epitope of hepatitis A virus (HAV) located on the VP3 capsid protein (110−121 peptide sequence, FW**RGD**LVFDFQV). Convalescent patient sera recognized the synthetic dodecapeptide, and also it cross-reacted with antiprotein antibodies and was able to induce antibodies that cross-reacted with the parent VP3 protein.

However, because not every residue of a continuous epitope necessarily makes contacts with the corresponding antibody and some of the residues can be replaced without impairing its antigenic reactivity.[3] In this direction, we investigated the effect of specific amino acid replacements on the RGD region, as well as deletions of the parent peptide, on its recognition by human convalescent sera. Only three single amino acid substitutions (RGE, RGK, and RGR) and one two amino acid substitution (AAD) conserved their recognition properties.[4]

In the absence of crystallographic data on the peptide−antibody complex, it is not clear whether such nonreplaceable residues actually interact with the antibody or whether they play an indirect role by acting as a scaffold to bring the neighboring residues at the required location for contacting the antibody. In any case, the ability of synthetic peptides to mimic specific recognition sites of antigenic proteins depends on sequential factors, as well as on conformational factors related to their sequences. Bearing in mind the fact that peptide−biomembrane interaction is an essential step of various kinds of bioactive peptides showing their function, we investigated the behavioral differences caused by the replacement of RGD by RGE (antigenic sequence) and RKD (nonantigenic sequence).

With the aim of characterizing the structural behavior of bioactive peptides in solution through different physicochemical techniques, we measured the surface activity of peptides [Glu^{114}]-VP3(110−121) and [Lys^{113}]VP3(110−121), analogues of the VP3(110−121) antigen of HAV.[5] Measurement of the surface activity of a molecule is a method used to estimate the molecular surface area, which in the case of flexible molecules can provide information about its conformational behavior.[5] In the physicochemical study mentioned above, the results obtained in the compression isotherms experiments showed that the lysine analogue exhibits a surface area about three times smaller than the glutamic acid analogue. These results were attributed to a differential conformational behavior of the two analogues in such a way that the latter analogue attains a more extended conformation than the former in the conditions of the experiment.[6]

To understand whether this observed differential conformational behavior of the two peptide analogues is a characteristic feature of the peptide sequences, we carried out molecular dynamics simulations of the two analogues in water. For this purpose, a 10 ns molecular dynamics simulation was performed on each of the two analogues. The comparative analysis of the molecular dynamics studies carried out are reported in the present work. The results of this study confirm a differential conformational behavior of the two peptides and provide support to the hypothesis of this observed behavior as the reason for the different surface areas obtained from compression isotherm experiments.

[†] Technical University of Catalonia.
[‡] IIQAB-CSIC.
[§] Universitat de Barcelona.

10.1021/jp022556+ CCC: $25.00
Published on Web 06/12/2003

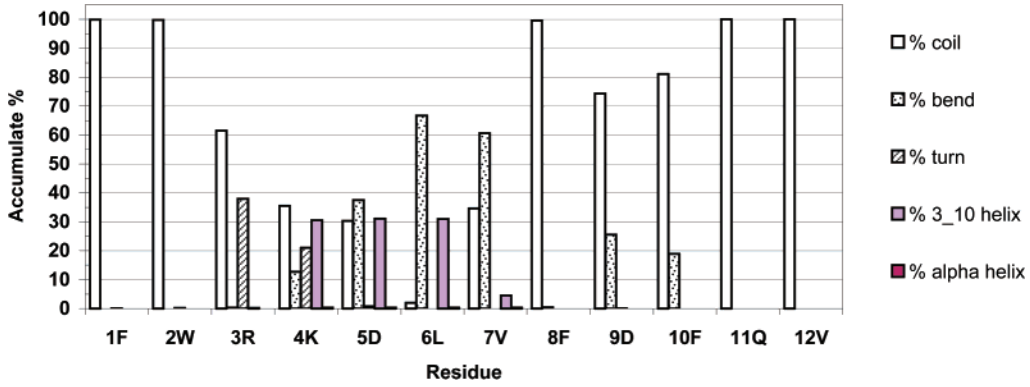

Figure 1. Percentage of the different secondary structures sampled by each of the residues of analogue [Lys^{113}]VP3(110−121) along the MD trajectory.

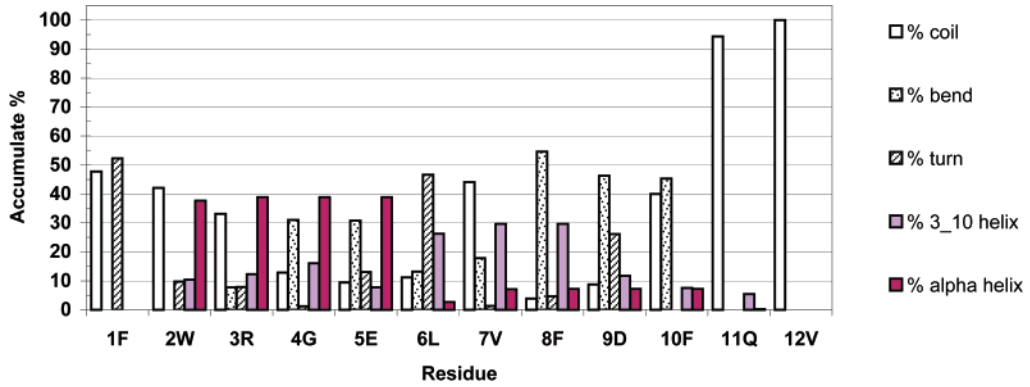

Figure 2. Percentage of the different secondary structures sampled by each of the residues of analogue [Glu^{114}]VP3(110−121) along the MD trajectory.

Methods

Compression Isotherms. Compression isotherms were performed using a Teflon trough (17 000 mm^2 surface area, 1 L volume). Peptide films were spread from chloroform solutions allowing at least 10 min for solvent evaporation. Films were compressed continuously with an area reduction rate of 60 mm^2/min. All samples were run at least three times in the direction of increasing pressure with freshly prepared films, obtaining a reproducibility of ±0.01 nm^2/molecule. The subphase temperature was 21 ± 0.5 °C. In addition, to assess the stability of the monolayers, the film was submitted to compression and decompression cycles.

Surface Activity Measurements. A Langmuir film balance KSV-5000 equipped with a Wilhelmy plate[7] was used. Surface activity measurements were carried out in a cylindrical trough (volume 70 mL) with mechanical stirring. The trough was filled with phosphate-buffered saline and increasing volumes of concentrated peptide solutions were injected directly underneath through a lateral hole. Pressure increases were recorded continuously for 120 min. Each run was carried out in triplicate, and reproducibility was usually within 0.1−0.2 mN/m.

Computer Simulations. A 10 ns molecular dynamics (MD) trajectory at 300 K was carried out with each of the two dodecapeptides using the AMBER5.0 program[8] with the Cornell all-atom force field.[9] Initial structures of the two molecules in their zwitterionic form were derived from their respective extended conformations after an initial energy minimization in vacuo using an effective dielectric constant of 80. The molecules were subsequently soaked in a box of TIP3P water molecules.[10]

MD trajectories were computed using periodic boundary conditions using a 10 Å cutoff for the nonbonded interactions and a constant relative dielectric constant $\epsilon = 1$. Hydrogens were frozen using the shake option, and the integration step was set to 0.2 fs. A. To keep the system at constant temperature, it was coupled to an external bath using the Berendsen's algorithm.[11] The systems were equilibrated during 100 ps in two steps. In the first 50 ps, the system was kept at constant volume, followed by 50 ps at constant pressure. After equilibration, an extra 10 ps step was carried out under the particle mesh Ewald conditions.[12,13] These calculations were performed with a spacing grid of 1 ± 0.1 Å on the three Cartesian axes, and a tolerance of 10^{-4} Å was set for the Ewald sums. Snapshots were collected every picosecond, resulting to a total of 10 000 structures stored for each system to perform structural analysis.

Results and Discussion

As described in ref 5, the two peptides are able to form stable monolayers that give regular isotherms on compression. Isotherms of the two analogues show the presence of the expanded and the liquid-condensed phases as the film is compressed with a low collapse pressure of 22 mN/m for the glutamic acid analogue and 29 mN/m for the lysine analog.[5] However, the isotherm of [Glu^{114}]VP3(110−121) exhibits an area per molecule about 3-fold larger than that exhibited by [Lys^{113}]VP3(110−121). Values of the area per molecule calculated at the collapse are 1.76 and 0.56 nm^2/molecule for the former and latter analogues, respectively, suggesting conformational differences between the two peptide analogues at the air/water interface.

Analysis of the adsorption process of the two peptides (from the subphase to the interface air/water) permits the computation of the surface excess (Γ) by means of eq 1. Results obtained, show that the surface excess of the lysine analogue is larger than that of the glutamic acid analogue, suggesting that the area of [Lys^{113}]VP3(110−121) is smaller than that of the other

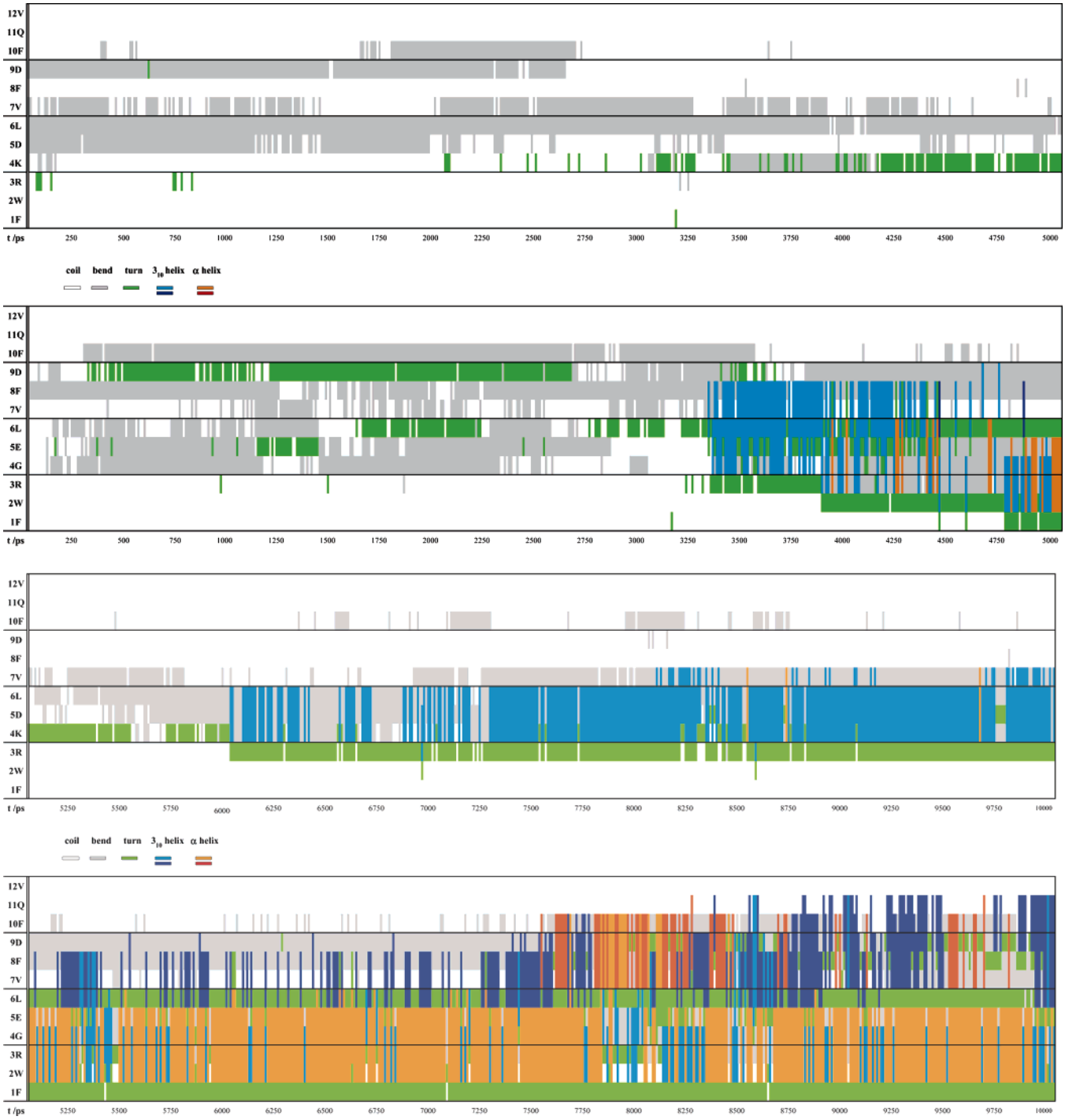

Figure 3. Diagrammatic representation of the secondary structure sampled by each of the residues of (a) analogue [Lys^{113}]VP3(110−121) and (b) analogue [Glu^{114}]VP3(110−121) along the MD trajectory.

peptide analogue (eq 2). For peptide concentrations of 0.1 μM, the area per molecule values calculated were 11.0 and 5.0 nm^2 for the glutamic acid and lysine analogues, respectively.

$$\Gamma = \frac{1}{RT}\frac{\Delta\Pi}{\Delta \ln c} \tag{1}$$

$$\text{area} = \frac{1}{\Gamma N} \tag{2}$$

where R is the gas constant (8.31 J/kmol), T is the temperature, $\Delta\Pi$ is the pressure increase achieved, c is the concentration, and N is Avogadro's number.

Molecular Dynamics Simulations. The total energy and the density of the systems were monitored during the trajectories. For [Glu^{114}] VP3(110−121), the total energy of the system was fairly constant at −10 278 kcal/mol with small fluctuations within 0.23% of this value. The mean value of the density was 0.992 g/cm^3 with the rmsd less than 0.29%. The total energy and density of [Lys^{113}]VP3(110−121) showed a similar behavior. Thus, the mean total energy of the system was −9977 kcal/mol with a rmsd value less than 0.23% and a mean value of the density of 0.994 g/cm^3 with a rmsd value less than 0.58%.

Secondary Structure Analysis. The secondary analysis of the peptides was carried out using 1 000 snapshots collected every 10 ps along the MD trajectories. Although the analysis could have been carried out using the 10 000 structures collected every picosecond, pilot calculations showed that the secondary

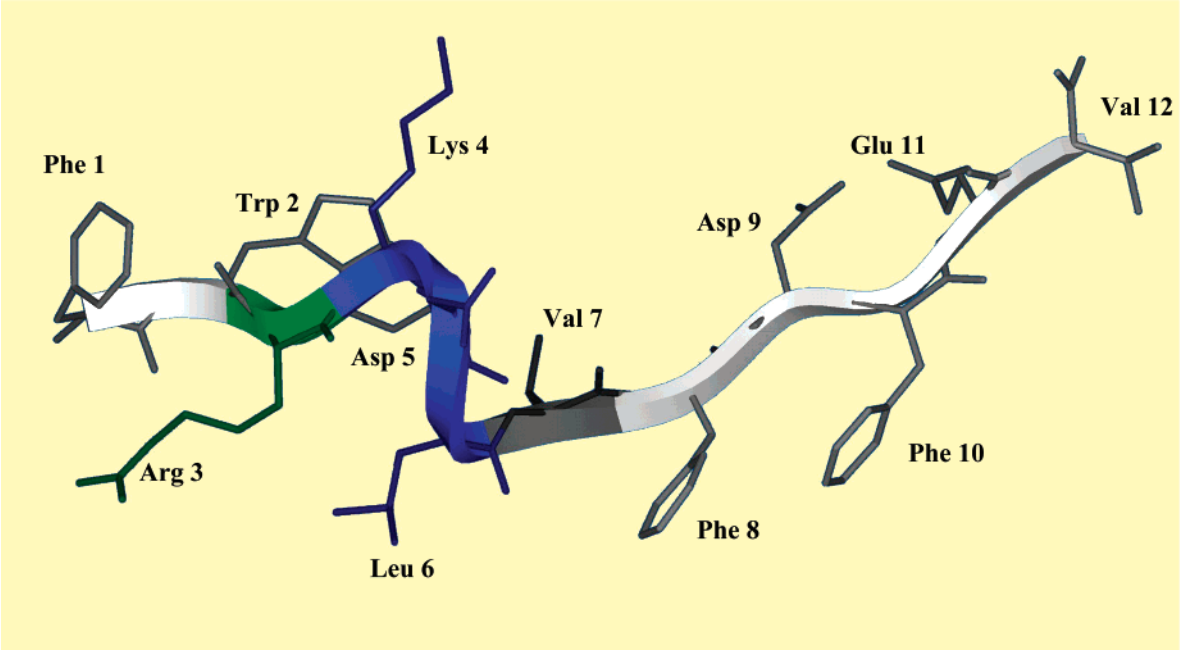

Figure 4. Ribbon representation of the most representative structure of analogue [Lys^{113}]VP3(110−121), exhibiting a 3_{10}-helical structure between residues 3 and 6, a turn at residue 3, and a bend at residue 7.

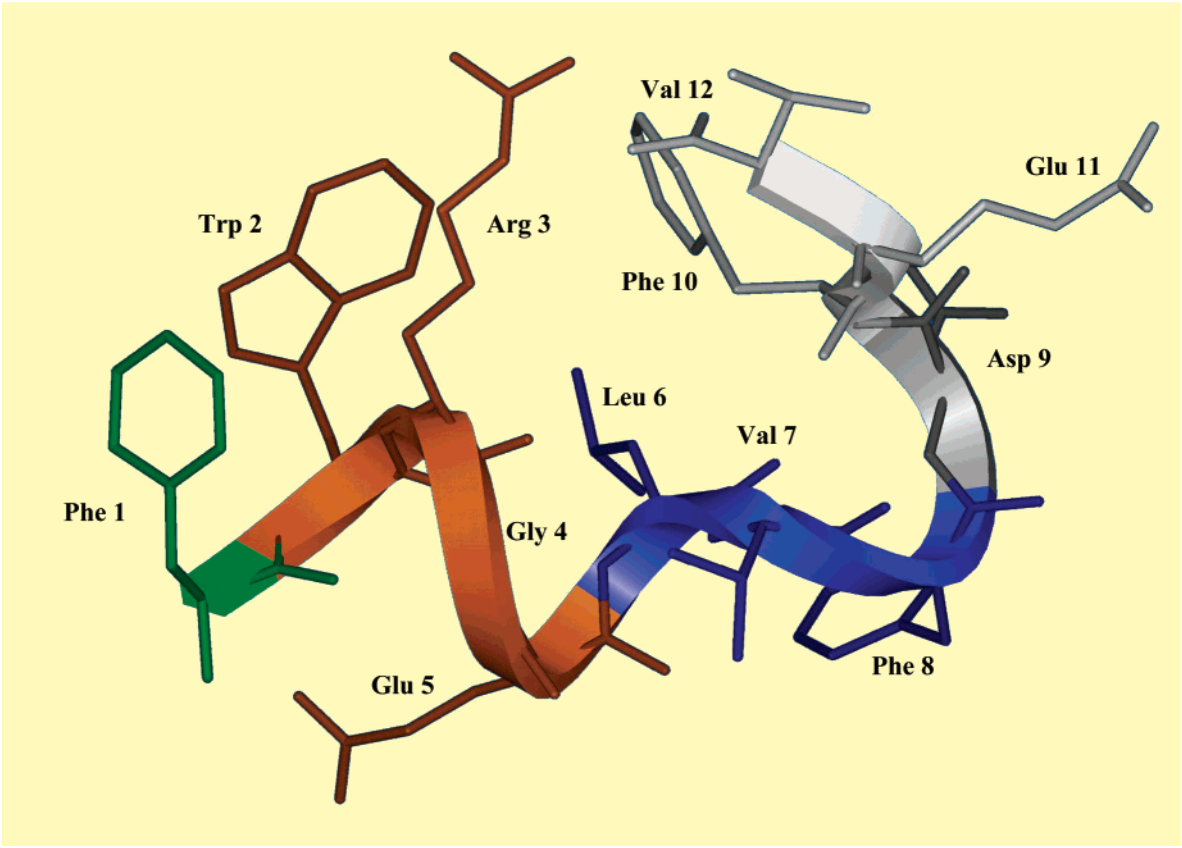

Figure 5. Ribbon representation of the most representative structure of analogue [Glu^{114}]VP3(110−121), exhibiting an α-helix between residues 2 and 5 and a 3_{10}-helical structure between residues 6 and 8.

motifs can be characterized with such a coarser sampling. Structural analysis was carried out using the program MOLMOD 2K.1[14] based on the secondary structure definitions of Kabsch and Sander.[15] Figures 1 and 2 show pictorially the results of the secondary structure analysis for each of the peptide analogues.

These results clearly suggest those residues actively involved in defining a secondary structure of the peptides. Moreover, it can be seen that there is a number of residues that exhibit either random coil or bend structures that cannot be considered as structuring elements of the peptide. Indeed, Figures 1 and 2 show a dramatic differential conformational behavior between the two peptides. Thus, whereas for [Lys^{113}]VP3(110−121) only residues located between 3 and 7 exhibit a high structuring profile, most of the residues of [Glu^{114}]VP3(110−121) participate extensively in the secondary structure of the peptide.

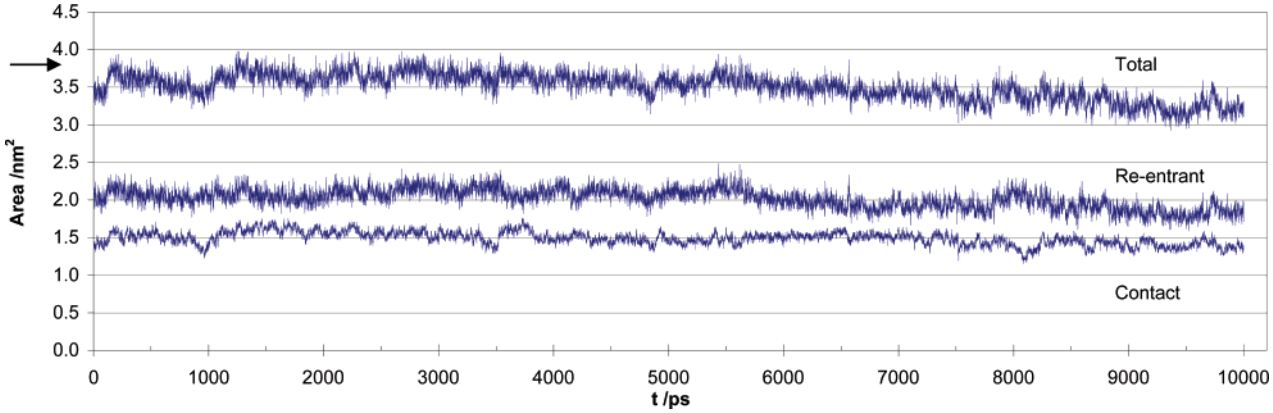

Figure 6. Evolution of the surface area of analogue [Lys[113]]VP3(110−121) during the MD trajectory.

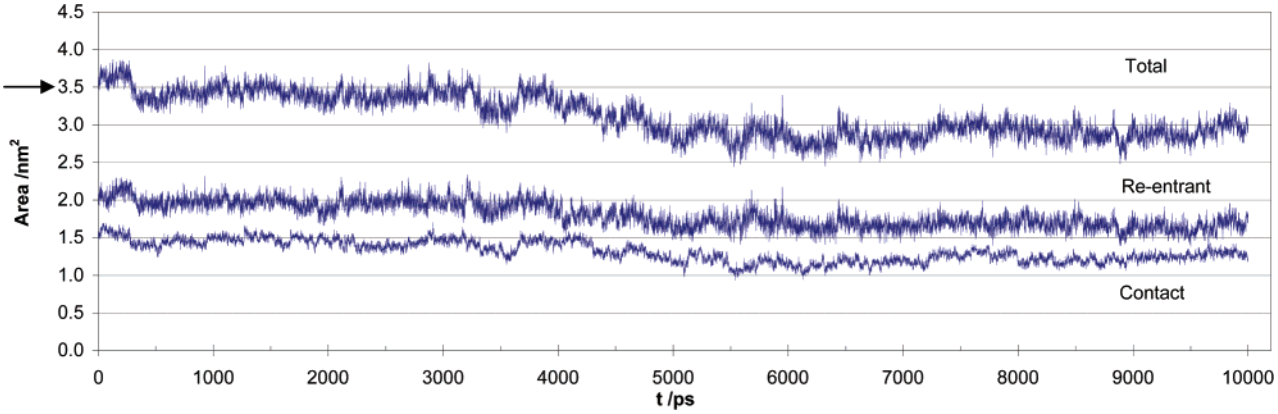

Figure 7. Evolution of the surface area of analogue [Glu[114]]VP3(110−121) during the MD trajectory.

Figure 3 shows the evolution of the secondary structure of the two peptides along the MD trajectory. In the case of [Lys[113]]VP3(110−121), a helix involving residues 4−6 is the basic secondary structure motif observed. The structure shows up for the first time after 6000 ps and appears to be stabilized after 7250 ps, its longest disappearance time being 50 ps after 9750 ps. The dynamic behavior of the molecule can be viewed as a fluctuating structure around this 3_{10} helix as the basic secondary structure of the peptide, extending its length sometimes to include residue 7 or evolving into an α-helix. Figure 4 shows a snapshot of the MD trajectory, showing the characteristic features of the secondary structure of the peptide including a 3_{10} helix between residues 4 and 6, a turn on residue 3, and a bend on residue 7.

A 3_{10} helix is also the most important secondary motif observed for [Glu[114]]VP3(110−121) appearing at 3250 ps, some time earlier than in the other analogue and consequently suggesting a higher tendency of the peptide to adopt folded structures. At 3900 ps, the helix is extended to include residue number 3. Later, the peptide attains an α-helix including an extra residue at each termini, to split up into two separate domains. After 4750 ps, the peptide adopts long standing structures, mainly the α-helix involving residues 2−5, which eventually fluctuates to a 3_{10} helix, a 3_{10} helix involving residues 6−8, which after 7500 ps can be extended to include residues 6−11 or adopt an α-helix involving residues 7−10. The most representative structure of this period is an α-helix including residues 2−5, together with either a 3_{10} helix between residues 6 and 9, an α-helix between residues 7 and 10, or a 3_{10} helix between residues 7 and 11, shown in Figure 5. In summary, a 3_{10} helix appears as the most commonly found structure that the peptide attains along the MD trajectory, although involving different residues, either 6−8, 4−6, or 4−8, the latter being the most frequently found.

TABLE 1: Effect of Solvation on the Accessible Surface Area of the Two Molecules

		contact area (nm²)	reentrant area (nm²)	total area (nm²)
[Glu[114]]VP3(110−121)	extended	1.56	1.92	3.48
	initial MD	1.48	2.09	3.58
[Lys[113]]VP3(110−121)	extended	1.74	2.01	3.75
	initial MD	1.42	2.13	3.55

Available Surface Calculation. The 10 000 snapshots collected were used to compute the accessible surface area of the two peptides during the trajectories. The solvent accessible surface area of the molecules was computed using Lee and Richards algorithm.[16] For these calculations, a 1.4 Å radius water probe was used and the atomic radii of the different atom types considered in the calculations were 1.7, 0.7, 1.5, 1.4 and 1.8 Å for C, H, N, O and S, respectively.

To monitor the effect of solvation on the accessible surface area, it was computed on the starting structure obtained after energy minimization and on the structure of the first snapshot of each trajectory. The results are shown in Table 1. These results suggest that the two molecules are sensitive to solvation. Interestingly, whereas [Glu[114]]VP3(110−121) appears to increase its total surface by about 3%, [Lys[113]]VP3(110−121) decreases it by about 5%. This observation agrees with the prediction of the grand average of hydropathicity (GRAVY),[17] being 0.358 for the former and 0.067 for the latter. However, it should also be taken into account that [Glu[114]]VP3(110−121) exhibits a net charge of −1, whereas [Lys[113]]VP3(110−121) is neutral.

The statistical analysis of the accessible surface area along the MD trajectories is shown in Table 2. The analysis suggests

TABLE 2: Statistics Results over the Two Sets of 10 000 Conformations Collected at the 10 ns of MD Simulation

	mean contact area (nm^2)	mean reentrant area (nm^2)	mean total area (nm^2)	initial value area (nm^2)
[Glu^{114}]VP3(110−121)	1.32 ± 0.14	1.80 ± 0.17	3.12 ± 0.29	3.58
[Lys^{113}]VP3(110−121)	1.49 ± 0.90	2.02 ± 0.13	3.51 ± 0.18	3.55

TABLE 3: Statistics Results of Accessible Surface over the Structuration Zone of MD Simulation

	mean contact area (nm^2)	mean reentrant area (nm^2)	mean total area (nm^2)	initial value area (nm^2)
[Glu^{114}]VP3(110−121)	1.25 ± 0.11	1.71 ± 0.13	2.96 ± 0.20	3.58
[Lys^{113}]VP3(110−121)	1.45 ± 0.83	1.91 ± 0.11	3.36 ± 0.14	3.55

that while [Glu^{114}]VP3(110−121) diminishes the contact surface with the solvent along the dynamics trajectory, [Lys^{113}]VP3(110−121) appears steady in a value slightly smaller than the value of the initial structure.

Figures 6 and 7 show the evolution of the accessible surface area along the MD trajectory. For [Glu^{114}]VP3(110−121), the accessible surface area exhibits four different features along the MD trajectory. Thus, during the first 250 ps, the peptide exhibits an accessible surface area higher than the one corresponding to the extended conformation. In the following period, until 3250 ps, the accessible surface area fluctuates around 3.5 nm^2. In a third period, until 5000 ps, the surface area experiences dramatic fluctuations with a net decrease to 0.5 nm^2. Finally, in the last period, the surface area fluctuates between 2.5 and 3.0 nm^2. [Lys^{113}]VP3(110−121) exhibits a different profile. During the first 100 ps, the peptide exhibits a value close to the initial, and after this period, the peptide evolves smoothly to attain a steady value of 3.0−3.5 nm^2. This differential behavior can be explained in terms of the secondary structure exhibited by the two analogues along the MD trajectories.

To obtain surface values that can be more easily compared to the experiment, it seems more interesting to compute the accessible surface area of the peptide once it has adopted a steady conformation. Thus, for [Lys^{113}]VP3(110−121), this can be carried out after 6000 ps and for [Glu^{114}]VP3(110−121) after 3310 ps. These calculations yield an average area of 3.4 nm^2 for the glutamic acid analogue and an average area of 3.0 nm^2 for the lysine analogue, as listed in Table 3. These values show the same trend of the experimental values of the collapse pressure of the two peptides. Thus, whereas for the glutamic acid analogue the molecular surface area is 1.76 nm^2/molecule (11 nm^2/molecule computed from surface activity measurements), the value drops dramatically to 0.52 nm^2/molecule (5 nm^2/molecule computed from surface activity measurements) in the case of the lysine analog.[6] This suggests that the observed behavior of the two analogues can be due to the intrinsic structural characteristics of the sequences of the two peptide analogues.

Conclusions

[Glu^{114}]VP3(110−121) and [Lys^{113}]VP3(110−121) are able to form stable monolayers when spread at an air/water interface, the isotherms of the former analogues being more expanded than those of the latter, thus indicating that not only the charge of the peptide but also the conformation of the peptide has to be considered. Moreover, from the peptides incorporation to the air/water interface analysis, lower area per molecule values were obtained for the [Lys^{113}]VP3(110−121) analogue.

Ten nanosecond long molecular dynamics simulations in water of the two HAV antigen peptide analogues, [Lys^{113}]VP3(110−121) and [Glu^{114}]VP3(110−121), have been carried out to determine whether there is an intrinsic differential conformational behavior of the two peptides. Analysis of the trajectories suggest that the lysine analogue exhibits a much higher degree of structure in solution.

Analysis of the total surface area of the two peptide analogues was also monitored along the MD trajectory. The two peptides exhibit similar average surface areas if this is computed along the whole trajectory. However, if the calculation is performed after the two peptides have adopted their secondary structures, the glutamic acid analogue exhibits a larger surface area than the lysine analogue. These results show the same trend as the results available from collapse surface area experiments, suggesting that the observed experimental behavior is due to an intrinsic structural nature of the peptides.

Acknowledgment. We are grateful to CESCA and CEPBA for a generous allocation of computer time granted to the project "Molecular Engineering". The Spanish Ministry of Science and Technology supported this work through Grant Numbers BIO95-0061 and PM98-0012-C02-01.

References and Notes

(1) Hancock, D. C.; O'Reilly, N. J.; Evan, G. I. *Mol. Biotechnol.* **1995**, *4*, 73.
(2) Van Regenmortel, M. H. V.; Muller, S. *Synthetic Peptides as Antigens*; Elsevier: Amsterdam, 1999; pp 1.
(3) Van Regenmortel, M. H. V. *Biologicals* **2001**, *29*, 209.
(4) Bosch, A.; González-Dankaart, J. F.; Haro, I.; Gajardo, R.; Pérez, J. A.; Pintó, R. M. *J. Med. Virol.* **1998**, *54*, 95.
(5) Sospedra, P.; Muñoz, M.; García, M.; Alsina, M. A.; Mestres, C.; Haro, I. *Biopolymers* **2000**, *54*, 477.
(6) Sospedra, P.; Mestres, C.; Haro, I.; Muñoz, M.; Busquets, M. A. *Langmuir* **2002**, *18*, 1231.
(7) Verger, R.; de Haas, G.H *Chem. Phys. Lipids* **1973**, *10*, 127.
(8) Case, D. A.; Pearlman, D. A.; Caldwell, J. W.; Cheatham, T. E., III; Wang, J.; Ross, W. S.; Simmerling, C.; Darden, T.; Merz, K. M.; Stanton, R. V.; Cheng, A.; Vincent, J. J.; Crowley, M.; Tsui, V.; Gohlke, H.; Radmer, R.; Duan, Y.; Pitera, J.; Massova, I.; Seibel, G. L.; Singh, U. C.; Weiner, P.; Kollman, P. A. *AMBER5.0*; University of California: San Francisco, CA, 1997.
(9) Cornell, W. D.; Cieplak, P.; Bayly, C. I.; Gould, I. R.; Merz, K. M., Jr.; Ferguson, D. M.; Spellmeyer, D. C.; Fox, T.; Caldwell, J. W.; Kollman, P. A. *J. Am. Chem. Soc.* **1995**, *117*, 5179.
(10) Jorgensen, W. L.; Chandrasekhar, J.; Madura, J. P. *J. Chem. Phys.* **1983**, *79*, 926.
(11) Berendsen, H. J. C.; Postma, J. P. M.; van Gunsteren, W. F.; DiNola, A.; Haak, J. R. *J. Chem. Phys.* **1984**, *81*, 3684.
(12) Darden, T. A.; York, D.; Pedersen, L. *J. Chem. Phys.* **1993**, *98*, 10089.
(13) Essman, U.; Perera, L.; Berkowitz, M. L.; Darden, T.; Lee, H.; Pedersen, L. G. *J. Chem. Phys.* **1995**, *103*, 8577.
(14) Koradi, R.; Billeter, M.; Wutrich, K. *J. Mol. Graphics* **1996**, *14*, 51.
(15) Kabsch, W.; Sander, C. *Biopolymers* **1983**, *22*, 2577.
(16) Lee, B.; Richards, M. *J. Mol. Biol.* **1971**, *55*, 379.
(17) Kyte, J.; Doolotle, R. F. *J. Mol. Biol.* **1982**, *157*, 105.